



PERGAMON

Available online at www.sciencedirect.com

SCIENCE @ DIRECT®

Polyhedron 22 (2003) 2557–2564



POLYHEDRON

www.elsevier.com/locate/poly

meta-Phenylene-bridged bis(imino nitroxide) biradicals as potential high-spin ligands

Takayuki Ichimura, Kentaro Doi, Chiemi Mitsuhashi, Takayuki Ishida*, Takashi Nogami

Department of Applied Physics and Chemistry, The University of Electro-Communications, Chofu, Tokyo 182-8585, Japan

Received 7 October 2002; accepted 14 January 2003

Abstract

Frozen-solution ESR spectra of 4-hydroxy-1,3-phenylenebis(imino nitroxide) (**1**) and 2-hydroxy-5-methyl-1,3-phenylenebis(imino nitroxide) (**2**) in toluene showed fine structures due to the triplet states (imino nitroxide stands for 2-substituted 4,4,5,5-tetramethylimidazolin-3-yloxy). The temperature dependence of the $\Delta m_s = \pm 2$ signal intensity for **1** followed the Curie law, suggesting that **1** has a ground triplet state. On the other hand, the triplet signal intensity of **2** did not obey the Curie law. The intramolecular magnetic coupling seems to depend on the twist angle between the imino nitroxide group and benzene ring. Complexation with $\text{Cu}(\text{CH}_3\text{CO}_2)_2 \cdot \text{H}_2\text{O}$ in ethanol gave a mononuclear complex, $\text{Cu}(\text{L}^1)_2$, where L^1 is the anionic form derived from **1**. The X-ray diffraction study of $\text{Cu}(\text{L}^1)_2$ revealed that the central copper(II) ion had a twisted square plane; the dihedral angle between two chelating O–Cu–N planes was 45° . The magnetic measurements of $\text{Cu}(\text{L}^1)_2$ indicated the presence of intramolecular ferromagnetic interaction, which is ascribed mainly to a ground quartet formation at the directly bonded radical–copper–radical moiety with $J_{\text{radical-copper}}/k_B = +132 \pm 5$ K, where the Heisenberg spin Hamiltonian is defined as $H = -2J\mathcal{S}_i\mathcal{S}_j$.

© 2003 Elsevier Science Ltd. All rights reserved.

Keywords: Ferromagnetic interaction; Nitroxide; Ligand; Free radical; ESR

1. Introduction

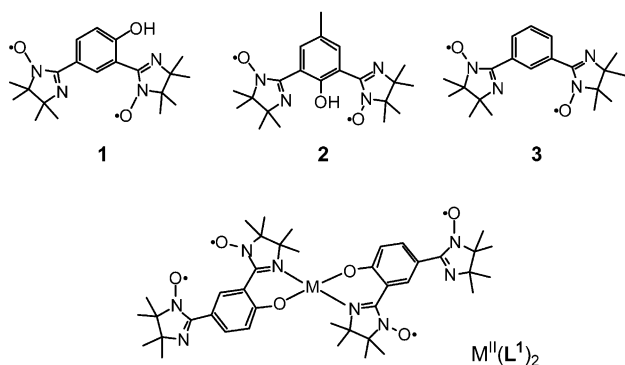
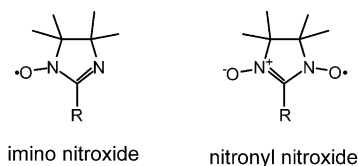
Polymeric complex formation containing transition metal ions and bridging radical ligands [1], especially high-spin oligoradical ligands [2], is supposed as an important strategy for constructing three-dimensional ferri- and ferromagnetic networks. In some case, large counter anions such as 1,1,1,5,5,5-hexafluoropentane-2,4-dionate (hfac) seem to be a hindrance against constructing strongly exchange-coupled systems [3], though the hfac salts facilitate the complex formation owing to the enhanced Lewis acidity of the metal ion. We will report here the synthesis and magnetic properties of 4-hydroxy-1,3-phenylenebis(imino nitroxide) (**1**) and 2-hydroxy-5-methyl-1,3-phenylenebis(imino nitroxide) (**2**) in order to exploit new high-spin (triplet)

ligands, where imino nitroxide denotes 2-substituted 4,4,5,5-tetramethylimidazolin-3-yloxy. The parent bis(imino nitroxide) (**3**) has recently been clarified to possess a ground triplet state by means of ESR and magnetic susceptibility measurements [4]. There have also been reports on the corresponding bis(nitronyl nitroxide) radicals (nitronyl nitroxide stands for 2-substituted 4,4,5,5-tetramethylimidazolin-3-yloxy-1-oxide) which reveals that the *meta*-phenylene spacer basically play a role of a ferromagnetic coupler [4–7], being consistent with the π -topological symmetry or spin-polarization scheme [8]. On the other hand, reports on the ground spin states of bis(imino nitroxides) are rare [4] and to our knowledge those of **1** and **2** are unknown so far. The central carbon atom in the nitronyl nitroxide ONCNO group has a node of the singly occupied molecular orbital (SOMO) because of the symmetry. The unsymmetric imino nitroxide ONCN group has a SOMO coefficient at the carbon atom, and the role of *m*-phenylene spacers may be modulated accordingly.

* Corresponding author. Tel.: +81-424-43-5490; fax: +81-424-43-5501.

E-mail address: ishi@pc.uec.ac.jp (T. Ishida).

Ligands L^1 and L^2 are planned to be derived from deprotonation of **1** and **2**. They are thought to possess the following advantages in pursuing high- T_C or T_N metal–radical magnets: (1) Chelation effect stabilizes coordination without hfac anions. (2) Anionic ligands L^1 and L^2 purge diamagnetic counter anions, which insulate magnetic networks. (3) Oligo-radicals have potential ability of forming three-dimensional networking structures owing to a multi-dentate character. We will also report here the crystal structure and magnetic properties of a mononuclear complex, $Cu(L^1)_2$, as a prototype for possible polymeric metal–radical hybrid solids.



2. Experimental

2.1. Materials

We prepared bis(nitronyl nitroxides) as precursors of **1–3** according to Ullman et al.'s method [9]. Condensation reaction of the corresponding diformylphenols with 2,3-bis(hydroxylamino)-2,3-dimethylbutane followed by oxidation with sodium metaperiodate gave bis(nitronyl nitroxide) biradicals. The resultant biradicals were deoxygenated with nitrous acid [10]. Treatment of the bis(nitronyl nitroxides) with sodium nitrite and acetic acid in dichloromethane afforded the corresponding bis(imino nitroxide) biradicals. The specimens suitable for ESR, magnetic measurements, and X-ray diffraction study were purified by passing a short column (silica gel eluted with 1/1 ethyl acetate–hexane) followed by repeated recrystallization from dichloromethane–hexane. Compound **1**: m.p. 119 °C (dec.), ESR (benzene, room temperature) $g = 2.0062$, $a_N = 4.4$, 2.2 G. A broad

dipolar signal overlapped the hyperfine structure. Compound **2**: m.p. 161–163 °C, ESR (benzene, room temperature) $g = 2.0062$, $a_N = 4.36$, 2.16 G. The observed hyperfine structure was well reproduced as a strongly exchanged “quintet of quintet” pattern. Compound **3** was satisfactorily analyzed with the literature data [4].

The following complexation procedure is typical. A methanol solution (1.3 ml) containing **1** (37 mg, 0.10 mmol) was added to a methanol solution (1.7 ml) containing $Cu(CH_3CO_2)_2 \cdot H_2O$ (10 mg, 0.05 mmol), and the combined solution was allowed to stand in a refrigerator overnight. Complex $Cu(L^1)_2$ was precipitated as black needles. Anal. Calc. for $C_{40}H_{54}N_8O_6Cu$ ($Cu(L^1)_2$): C, 59.57; H, 6.75; N, 13.90. Found: C, 59.59; H, 6.63; N, 13.58%.

2.2. Instruments

X-ray diffraction data of single crystals were collected on a Rigaku R-axis RAPID diffractometer with graphite monochromated Mo $K\alpha$ ($\lambda = 0.71069$ Å) radiation for **1** and Cu $K\alpha$ ($\lambda = 1.5418$ Å) radiation for $Cu(L^1)_2$ at 100 K. The structures were solved by direct methods and expanded using Fourier techniques in the TEXSAN program package [11]. Numerical absorption correction was used. The thermal displacement parameters were refined anisotropically for non-hydrogen atoms. Hydrogen atoms were located at the calculated positions for $Cu(L^1)_2$ and a disordered portion in **3**. Full-matrix least-squares methods were applied using all of the unique diffraction data.

ESR spectra were recorded on a Bruker ESP300E X-band (9.7 GHz) spectrometer equipped with an Oxford cryostat for low-temperature measurements. Saturation effects were carefully removed from the spectra by lowering the microwave power. Simulated spectra for the frozen and liquid solutions were calculated in the WINEPR SIMFONIA program [12].

Magnetic susceptibilities of polycrystalline samples were measured on a Quantum Design MPMS SQUID magnetometer equipped with a 7 T coil in a temperature range 1.8–300 K. The magnetic responses were corrected with diamagnetic blank data of the sample holder obtained separately. The diamagnetic contribution of the sample itself was estimated from Pascal's constants.

3. Results and discussion

3.1. Molecular and crystal structures

The molecular and crystal structures of **1** are shown in Fig. 1. Selected crystallographic parameters are listed in Table 1. The crystal structure was solved in an orthorhombic $Pbca$ space group. All of the hydrogen atoms were experimentally found. The molecules are

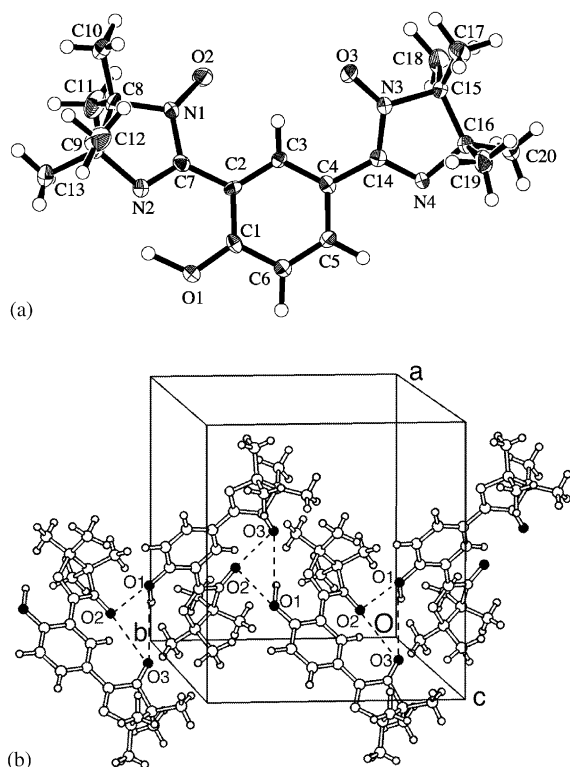


Fig. 1. (a) Ortep drawing of **1** with thermal ellipsoids at the 50% level for non-hydrogen atoms. (b) Molecular arrangements in the crystal of **1**. The oxygen atoms are darkened. The interatomic distances of $O1 \cdots O2\#$ and $O1 \cdots O3\#$ are 3.276(3) Å and 3.746(4) Å, respectively, where the symmetry operation code of # is $-x+3/2, y-1/2, z$.

Table 1
Crystallographic parameters of **1** and $Cu(L^1)_2$

Compounds	1	$Cu(L^1)_2$
Empirical formula	$C_{20}H_{28}N_4O_3$	$C_{40}H_{54}N_8O_6Cu_1(H_2O)_2$
Habit	red block	black block
Crystal system	orthorhombic	monoclinic
Space group	<i>Pbca</i>	<i>P2₁/c</i>
<i>a</i> (Å)	13.0055(4)	12.630(3)
<i>b</i> (Å)	12.1683(4)	14.160(4)
<i>c</i> (Å)	24.954(1)	24.700(6)
β (°)	90.	93.645(6)
<i>V</i> (Å ³)	3949.1(4)	4408(1)
<i>Z</i>	8	4
<i>D</i> _{calc} (g cm ⁻³)	1.253	1.215
λ (Å)	0.71069	1.5418
<i>T</i> (K)	100	100
Reflections	3547	3457
<i>R</i> (<i>F</i> ²) (<i>I</i> > 2σ(<i>I</i>))	0.0989	0.0688
<i>R</i> _w (<i>F</i>) (all data)	0.196	0.164

almost planar with respect to the π -conjugation system, as indicated by the dihedral angles between imidazoline and benzene rings (23.1(1)° and 8.0(1)° for the imino nitroxide groups at the 2- and 4-positions, respectively). An intramolecular hydrogen bond is found among the $O1-H \cdots N2$ moiety, forming an almost planar six-membered ring.

As Fig. 1(b) shows, the intermolecular short contacts were found between hydroxyl oxygen and imino nitroxide oxygen atoms within 3.3 Å. Hydrogen bonding is an important factor for the crystal engineering and is also proposed to provide a magnetic coupling pathway [13–15]. A linear molecular arrangement of the molecule of **1** can be found along the *b*-axis with the $O1-H \cdots O2$ and $O1-H \cdots O3$ hydrogen bonds. Magnetic measurements of the crystal of **1** (see below) suggest that the intermolecular magnetic interactions through the hydrogen bonds (Fig. 1(b)) might be antiferromagnetic.

Unfortunately, **2** did not afford good crystals for the X-ray diffraction study. The crystal structure of **3** was satisfactorily analyzed and reproduced the results previously reported [4]. We collected the diffraction data at 100 K and intermolecular short contacts are precisely determined to be 3.30 and 3.33 Å for $O \cdots N$ and $O \cdots O$ at the nearest NO groups (Fig. 2), which are close to the sum of the van der Waals radii (ca. 3 Å). Consequently we can propose that the crystal of **3** consists of an antiferromagnetically correlated dimer.

In the course of our attempts to prepare transition metal ion complexes containing L^1 and L^2 , $Cu(L^1)_2$ was obtained as single crystals, while $Co(L^1)_2$, $Ni(L^1)_2$, and $Zn(L^1)_2$ only as fine powder forms. Fig. 3 shows the molecular structure of $Cu(L^1)_2$. Selected crystallographic parameters are listed in Table 1 and important geometrical parameters are in Table 2. Complex $Cu(L^1)_2$ is mononuclear; outer imino nitroxide groups are free from metal coordination and no meaningful interatomic contacts were found among molecules. The thermal displacement factors of methyl groups were somewhat large even at 100 K, probably due to the presence of conformational isomers. However, disorder models did not improve the *R* factor.

The copper ion has an intermediate geometry between a square-planar structure and a tetrahedral one. Two chelating planes are canted each other, forming a dihedral angle of 45° between two planes of $O1-Cu1-N2$ and $O4-Cu1-N6$. Kahn, Luneau, and their co-workers clearly demonstrated that the orthogonal ar-

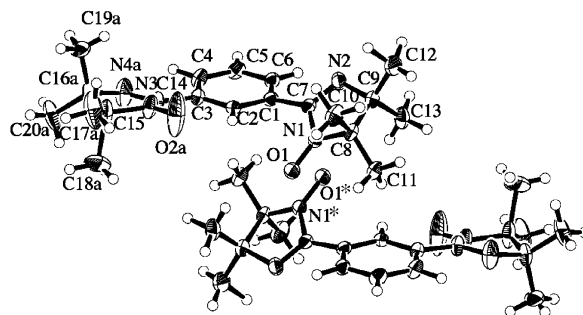


Fig. 2. Ortep drawing of two neighboring molecules of **3** with thermal ellipsoids at the 50% level. Only a major conformation is drawn. Interatomic distances are: $O1 \cdots N1^*$, 3.302(3) Å; $O1 \cdots O1^*$, 3.327(5) Å. The symmetry operation code for * is $-x+1, -y, -z+1$.

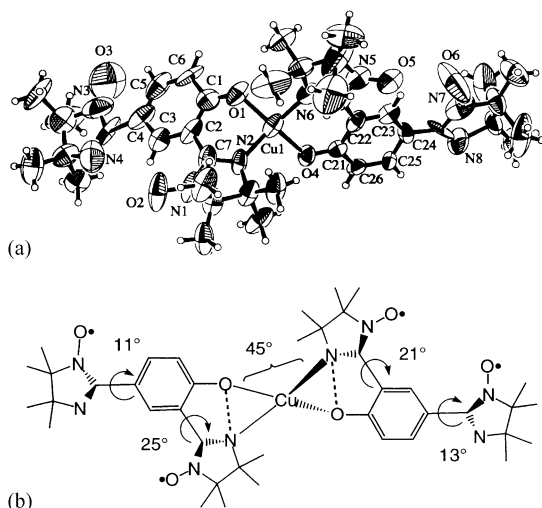


Fig. 3. (a) Ortep drawing of $\text{Cu}(\text{L}^1)_2$ with thermal ellipsoids at the 30% level. (b) Selected dihedral angles.

Table 2

Selected bond lengths (Å) and angles ($^\circ$) in $\text{Cu}(\text{L}^1)_2$

Bond lengths

Cu(1)–O(1)	1.905(5)
Cu(1)–O(4)	1.874(5)
Cu(1)–N(2)	1.980(8)
Cu(1)–N(5)	2.015(8)
O(1)–C(1)	1.30(1)
O(2)–N(1)	1.28(1)
O(3)–N(3)	1.20(2)
N(2)–C(7)	1.29(1)
O(4)–C(21)	1.27(1)
O(5)–N(5)	1.293(9)
N(5)–C(27)	1.40(1)
O(6)–N(7)	1.32(2)

Bond angles

O(1)–Cu(1)–O(4)	148.3(3)
O(1)–Cu(1)–N(2)	92.0(3)
O(1)–Cu(1)–N(6)	99.0(3)
O(4)–Cu(1)–N(2)	94.3(3)
O(4)–Cu(1)–N(6)	92.1(3)
N(2)–Cu(1)–N(6)	147.5(3)
Cu(1)–O(1)–C(1)	127.3(7)
Cu(1)–N(2)–C(7)	121.9(7)
Cu(1)–O(4)–C(21)	128.3(6)
Cu(1)–N(6)–C(27)	122.6(8)
N(6)–C(27)–C(22)	124(1)
N(2)–C(7)–C(2)	126(1)

rangement between two magnetic orbitals, an organic π -spin and an inorganic $d\sigma$ -spin, led to ferromagnetic coupling in radical–metal compounds such as the high-spin *o*-semiquinone–copper(II) complex [16] and 2-pyridyl imino nitroxide complexes containing copper(II) and nickel(II) ions [17]. In the present study, assuming that the imino nitrogen atom carrying a radical π -spin is directly bonded to the copper(II) ion at the equatorial position where the $d_{x^2-y^2}$ magnetic orbital resides, we

can expect ferromagnetic coupling between the π and d spins and consequently a local high-spin ($S = 3/2$) in the radical–copper–radical moiety.

Each L^1 moiety has a less coplanar π -conjugation system than those of **1**. The dihedral angles are shown in Fig. 3(b). Furthermore, the directions of the unsymmetrical ONCN groups are different between **1** and L^1 ; the ONCN groups of **1** are arranged in a head-to-head manner, i.e., two oxygen atoms were closely located (Fig. 1(a)), whereas the ONCN groups are in a head-to-tail manner for one biradical portion of $\text{Cu}(\text{L}^1)_2$.

3.2. ESR spectra

We measured frozen-solution ESR spectra of **1**–**3** in toluene. Fig. 4 shows fine structures for **1** and **2**. The spectrum of **1** clearly exhibits six transition lines together with a central doublet signal as an impurity. The width between the most outer signals corresponds to a zero-field splitting parameter $|2D'|$ and the distance between the dipoles was calculated to be 5.1 Å from $|D'| = 204$ G. The X-ray crystallographic analysis revealed that two imino nitroxide oxygen atoms were closely located with the $\text{O}2 \cdots \text{O}3$ distance of 3.944 (4) Å. Viewing from spin delocalization on the ONCN π -system, the distance between the spins is better estimated from that of $\text{C} \cdots \text{C}$ than that of $\text{O} \cdots \text{O}$. The $\text{C}7 \cdots \text{C}14$ distance is 5.028 (5) Å, which is very close to the value

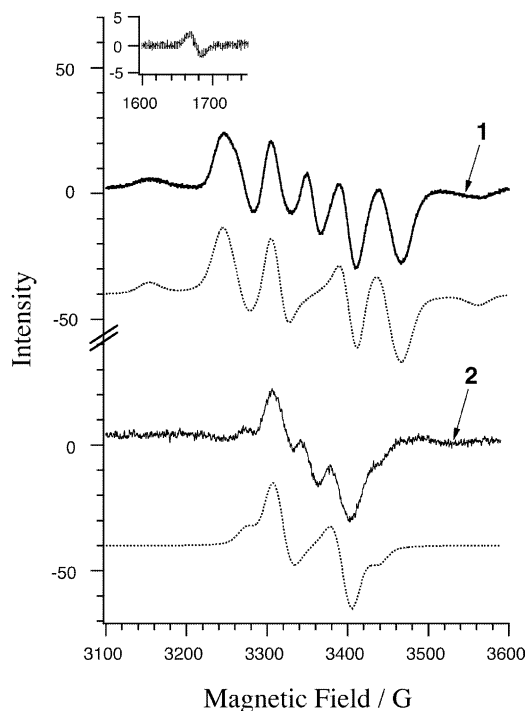


Fig. 4. Frozen solution ESR of **1** (10.8 K) and **2** (11.2 K) in toluene. The $\Delta m_s = \pm 2$ transition signal in a half-field region for **1** is shown in the inset. Simulated spectra were shown with dotted lines. For the optimized parameters, see the text.

calculated above. Another parameter $|E'|$ was estimated to be small (ca. < 5 G) which could not be precisely determined, because the spectrum consists of two fine structures, probably due to the presence of another molecular conformation. The $|D'|$ value of the second conformer was 94 G, which is close to that of **3** (92 G in toluene; 90 G in xylene-dichloromethane [4]). The approximate dipole–dipole distance is calculated to be 6.8 Å, which is ascribable to a conformer with two NO groups apart by flipping the imino nitroxide ring by about 180°. The simulated spectrum of **1** in Fig. 4 was drawn as the sum of two components.

A forbidden ($\Delta m_s = \pm 2$ transition) signal was found near a half field (1670 G) for **1**, as shown in the inset of Fig. 4. The temperature dependence of the $\Delta m_s = \pm 2$ signal obeys the Curie law, $I_{\text{ESR}} = C/T$, where C is an arbitrary constant (Fig. 5). The ground spin multiplicity of **1** is suggested to be triplet. Turek and coworkers [4] reported that the parent bis(imino nitroxide) (**3**) also had a triplet ground state. These results are consistent with the general rule that the *m*-phenylenes serve as robust ferromagnetic couplers [8]. However, it is not completely eliminated that the singlet and triplet states are almost degenerate. Actually, the singlet–triplet gap of **3** was estimated as small as $J/k_B = 10 \pm 5$ K [4], and the phenolic hydroxyl group tends to reduce the ferromagnetic J values compared with a non-substituted biradical [7].

On the other hand, no forbidden signal was observed in the ESR spectra of **2**. The zero-field splitting parameters are: $|D'| = 82$ G and $|E'| < 5$ G. The $|D'|$ value is smaller than those of **1** and **3**, suggesting the spins in **2** are rather localized at the two imino nitroxide groups. Although the crystallographic analysis of **2** was unsuccessful, we suppose that the π -conjugation system of **2** is not a coplanar owing to the steric congestion at neighboring two imino nitroxide and a hydroxyl groups.

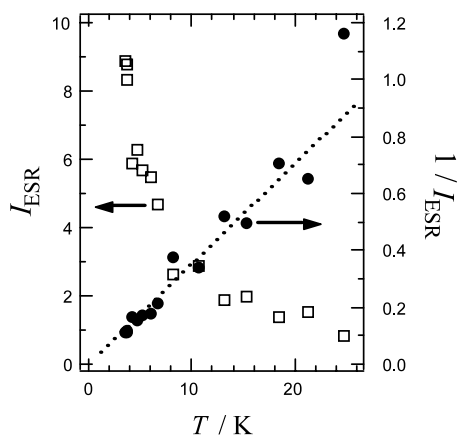


Fig. 5. Temperature dependence of I_{ESR} (left axis) and $1/I_{\text{ESR}}$ (right axis) for **1**. The ESR signal intensity (I_{ESR}) was defined by the peak height of the signal integral due to the $\Delta m_s = \pm 2$ transition. A dotted line is shown for a guide to the eye.

We examined the temperature dependence of the signal intensity of the triplet fine structure, and found that the intensity of the signal at 3320 G did not obey the Curie law. Assuming that the imino nitroxide and benzene rings in **2** are not conjugated practically, violation of the general rule is conceivable. Steric effects are known to give rise to stabilization of the singlet state for some *m*-phenylene-bridged bis(*t*-butyl nitroxide) radicals [18]. Such conformational effects may also hold for bis(imino nitroxide) radicals, as suggested from the computational analysis [4,19].

3.3. Magnetic properties

The results of the magnetic measurements on the polycrystalline samples of **1–3** are shown in Fig. 6. For all compounds, the products of the molar magnetic susceptibility (χ_{mol}) and T decrease on lowering temperature. The theoretical $\chi_{\text{mol}}T$ value of the high-temperature limit is $0.75 \text{ cm}^3 \text{ K mol}^{-1}$ and agrees well the experimental values at 300 K.

A stepwise behavior was found for **3**, which reproduces the result recently reported [4]. Analysis of the data on **3** may afford a valuable information. Intra- and intermolecular exchange coupling parameters, J_{intra} and J_{inter} , are defined as illustrated in Fig. 7, since the X-ray crystallographic analysis suggested the dimer formation in the crystal of **3** (Fig. 2). The best fit to the four-spin model [20] gave $J_{\text{intra}}/k_B = +20 \pm 1$ K and $J_{\text{inter}}/k_B = -88 \pm 3$ K, where the Heisenberg spin Hamiltonian is defined as $H = -2JS_iS_j$. A calculated curve is satisfactorily superposed to the experimental data as shown in Fig. 6, and the present result is essentially the same as the reported one [4]. It is noteworthy that the intermolecular antiferromagnetic coupling is much larger than the intramolecular ferromagnetic one and that the

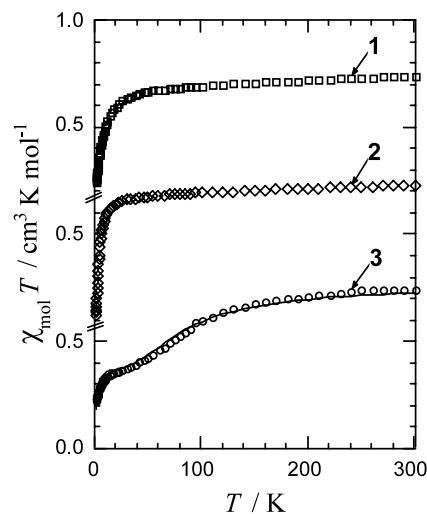


Fig. 6. Temperature dependence of the product of χ_{mol} and T measured at 5 kOe for **1–3**. The solid line represents a theoretical fit for **3** based on a dimeric four-spin system. For details, see the text.

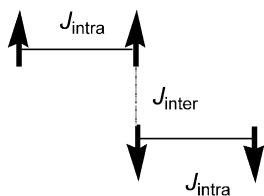


Fig. 7. Four-spin model proposed for **3** based on the X-ray crystallographic analysis.

latter is buried in the former, giving only the $\chi_{\text{mol}}T$ decrease on cooling.

The featureless decreases of $\chi_{\text{mol}}T$ of **1** and **2** leave no reliable analysis based on appropriate spin–spin coupling models. Apparent Weiss temperatures (θ) are determined to be -4.3 and -2.6 K for **1** and **2**, respectively, from the Curie–Weiss analysis ($\chi_{\text{mol}} = C/(T - \theta)$). No ferromagnetic behavior could be found in Fig. 6, but we can more cautiously conclude that the ferro- or antiferromagnetic interaction across the *m*-phenylene bridge should be smaller than the order of θ , if any, because antiferromagnetic intermolecular interactions may bury the intramolecular ferromagnetic interactions, as suggested from the results of **3**.

Magnetic susceptibility measurements on $\text{Cu}(\text{L}^1)_2$ revealed the role of *m*-phenylene bridge in L^1 as magnetic couplers; the L^1 has a nominal anionic charge which may bring about a magnetic role different from that of **1**. Fig. 8 shows the temperature dependence of the $\chi_{\text{mol}}T$ value of $\text{Cu}(\text{L}^1)_2$. With a decrease of temperature, the $\chi_{\text{mol}}T$ value once increased, reached a maximum of $2.65 \text{ cm}^3 \text{ K mol}^{-1}$ around 30 K, and then decreased. Although the increase of $\chi_{\text{mol}}T$ indicates the presence of ferromagnetic interaction, the experimental value was much smaller than the value of $4.38 \text{ cm}^3 \text{ K mol}^{-1}$ expected for a possible highest $S = 5/2$ state. The maximum value corresponds to a theoretical value of

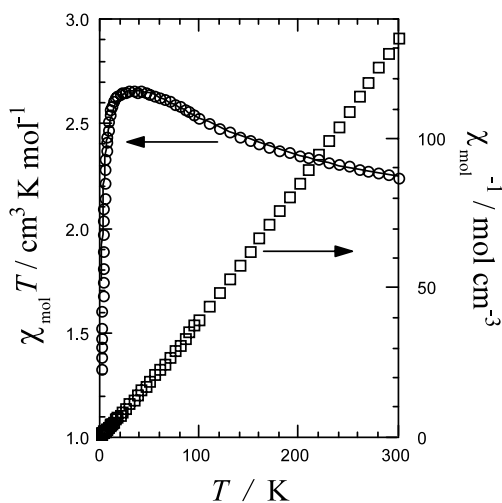
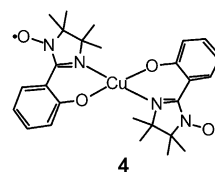


Fig. 8. Temperature dependence of the product of χ_{mol} and T measured at 5 kOe for $\text{Cu}(\text{L}^1)_2$. The solid line represents a theoretical fit. For details, see the text.

$2.63 \text{ cm}^3 \text{ K mol}^{-1}$ expected for the sum of paramagnetic spins of two $S = 1/2$ and one $S = 3/2$ in a whole molecule. Thus, the increase of $\chi_{\text{mol}}T$ observed on cooling from 300 to 30 K can be ascribed mainly to the ferromagnetic coupling at the central radical–copper–radical moiety. This interpretation is rationalized by the fact that the magnetic coupling at directly bonded radical–copper system is considerably large. Actually, the high-spin *o*-semiquinone–copper(II) complex have a ferromagnetic coupling with $J/k_{\text{B}} = 160$ K [16], and the 2-pyridyl imino nitroxide–copper(II) complex with $J/k_{\text{B}} > 210$ K [17]. Very recently, Okada and Kaizaki independently studied the magnetic properties of **4** [21], which can be regarded as a model compound of the central portion of $\text{Cu}(\text{L}^1)_2$. According to their preliminary reports, **4** has a ground quartet state with ferromagnetic interaction of the order of 10^2 K.



We analyzed the magnetic data on $\text{Cu}(\text{L}^1)_2$ using the following equation derived from the spin–pin Hamiltonian $H = -2J(S_1S_2 + S_2S_3)$ based on the model illustrated in Fig. 9:

$$\chi_{\text{mol}}T = \frac{N_{\text{A}}\beta^2g^2}{2k_{\text{B}}} \times \left[1 + \frac{\exp(-2J/k_{\text{B}}T) + 1 + 10 \exp(J/k_{\text{B}}T)}{2 \exp(-2J/k_{\text{B}}T) + 2 + 4 \exp(J/k_{\text{B}}T)} \right] \times \frac{T}{T - \theta}$$

Here, J is defined as a coupling parameter for both sides of the radical–copper interactions since the molecule is almost symmetrical. Possible magnetic couplings across the *m*-phenylene bridges as well as intermolecular couplings are confined to a Weiss mean field parameter θ . The parameters were optimized as $J/k_{\text{B}} = 132 \pm 5$ K, $\theta = -1.0 \pm 0.2$ K, and $g = 2.06 \pm 0.01$, and the calculated curve is superposed in Fig. 8. The data are satisfactorily fit, indicating that the model proposed is reliable. In spite of the distorted six-membered chelate ring and twisted two chelate rings, considerably large ferromagnetic coupling takes place between the radical and copper(II) spins. The ferro- or antiferromagnetic interaction across the *m*-phenylene

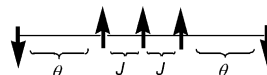


Fig. 9. A model containing a three-spin system plus two doublets proposed for $\text{Cu}(\text{L}^1)_2$ based on the X-ray crystallographic analysis.

bridge should be smaller than the order of θ . Therefore, we can conclude that the *m*-phenylene bridges work as not so strong ferromagnetic couplers in \mathbf{L}^1 .

4. Summary

Although ESR is a versatile technique for determination of the spin-multiplicity of the molecule, we usually have to attention to the difference between molecular structures especially conformational isomerism in solid states and in solutions. The frozen-solution ESR results on $\mathbf{1}$ suggest that the ground state of $\mathbf{1}$ is triplet, whereas the solid-state magnetic susceptibility results on $\mathbf{1}$ and $\text{Cu}(\mathbf{L}^1)_2$ revealed that the *m*-phenylene bridges hardly worked as ferromagnetic couplers. This discrepancy may originate in conformational isomerism due to the steric effects of adjacent substituents as well as in electronic perturbation also due to the effects of substituents, such as hydroxyl and anionic phenolate groups. Taking all the results obtained here into consideration, *m*-phenylene-bridged bis(imino nitroxide) biradicals are not so good candidates in pursuit of high-spin ligands in contrast to our initial expectation, because the ferromagnetic interaction across the *m*-phenylene is a few kelvins at the most. However, we have clarified that the chelate structure of copper(II) *o*-imino nitroxide-substituted phenolates is available as a potential high-spin building block with considerably large ferromagnetic exchange coupling in the development of metal–radical hybrid magnets.

5. Supplementary material

Crystallographic data for the structural analysis(excluding structure factors) have been deposited with the Cambridge Crystallographic Data Centre, CCDC Nos. 194642 and 194643 for the compounds $\mathbf{1}$ and $\text{Cu}(\mathbf{L}^1)_2$, respectively. Copies of this information may be obtained free of charge from The Director, CCDC, 12 Union Road, Cambridge CB21 EZ, UK (fax: +44-1223-336033, e-mail: deposit@ccdc.cam.ac.uk or www: <http://www.ccdc.cam.ac.uk>).

Acknowledgements

This work was supported by a Grant-in-Aid for Scientific Research on Priority Areas of “Molecular Conductors and Magnets” (No. 730/11224204) and by a Grant-in-Aid for Scientific Research (No. 13640575), both from the Ministry of Education, Culture, Sports, Science and Technology, Japan.

References

- [1] (a) A. Caneschi, D. Gatteschi, P. Rey, R. Sessoli, *Acc. Chem. Res.* 22 (1989) 392; (b) H.O. Stumpf, L. Ouahab, Y. Pei, D. Grandjean, O. Kahn, *Science* 261 (1993) 447; (c) J.S. Miller, A.J. Epstein, *Angew. Chem., Int. Ed. Engl.* 33 (1994) 385; (d) W. Fujita, K. Awaga, M. Takahashi, M. Takeda, T. Yamazaki, *Chem. Phys. Lett.* 362 (2002) 97.
- [2] (a) K. Inoue, T. Hayamizu, H. Iwamura, D. Hashizume, Y. Ohashi, *J. Am. Chem. Soc.* 118 (1996) 1803; (b) H. Iwamura, K. Inoue, T. Hayamizu, *Pure Appl. Chem.* 68 (1996) 243.
- [3] A. Caneschi, P. Chiesi, L. David, F. Ferraro, D. Gatteschi, R. Sessoli, *Inorg. Chem.* 32 (1993) 1445.
- [4] L. Catala, J. Le Moigne, N. Kyritsakas, P. Rey, J.J. Novoa, P. Turek, *Chem. Eur. J.* 7 (2001) 2466.
- [5] (a) A. Izuoka, M. Fukuda, T. Sugawara, *Mol. Cryst. Liq. Cryst.* 232 (1993) 103; (b) A. Izuoka, R. Kumai, T. Sugawara, *Adv. Mater.* 7 (1995) 672; (c) D. Shiomi, M. Tamura, H. Sawa, R. Kato, M. Kinoshita, *J. Phys. Soc. Jpn.* 62 (1993) 289.
- [6] D. Shiomi, M. Nishizawa, K. Kamiyama, S. Hase, T. Kanaya, K. Sato, T. Takui, *Synth. Met.* 121 (2001) 1810.
- [7] (a) S. Hase, D. Shiomi, K. Sato, T. Takui, *Polyhedron* 20 (2001) 1403; (b) S. Hase, D. Shiomi, K. Sato, T. Takui, *J. Mater. Chem.* 11 (2001) 756.
- [8] (a) H. Iwamura, *Adv. Phys. Org. Chem.* 26 (1990) 179; (b) J. Veciana, H. Iwamura, *MRS Bull.* 25 (2000) 41; (c) A. Rajca, *Chem. Rev.* 94 (1994) 871; (d) J.A. Crayston, J.N. Devine, J.C. Walton, *Tetrahedron* 56 (2000) 7829.
- [9] E.F. Ullman, J.H. Osiecki, D.G.B. Boocock, R. Darcy, *J. Am. Chem. Soc.* 94 (1972) 7049.
- [10] E.F. Ullman, L. Call, J.H. Osiecki, *J. Org. Chem.* 35 (1970) 3623.
- [11] TEXSAN: Crystal Structure Analysis Package, Molecular Structure Corp., The Woodlands, TX, 1985, 1999.
- [12] Bruker WINEPR SIMFONIA, 1.25, shareware version, Bruker Analytical Instruments, Rheinstetten, Germany, 1996.
- [13] (a) T. Sugawara, M.M. Matsushita, A. Izuoka, N. Wada, N. Takeda, M. Ishikawa, *J. Chem. Soc., Chem. Commun.* (1994) 1723; (b) M.M. Matsushita, A. Izuoka, T. Sugawara, T. Kobayashi, N. Wada, N. Takeda, M. Ishikawa, *J. Am. Chem. Soc.* 119 (1997) 4369; (c) J. Cirujeda, M. Mas, E. Molins, F.L. de Panthou, J. Laugier, J.G. Park, C. Paulsen, P. Rey, C. Rovira, J. Veciana, *J. Chem. Soc., Chem. Commun.* (1995) 709; (d) E. Hernandez, M. Mas, E. Molins, C. Rovira, J. Veciana, *Angew. Chem., Int. Ed. Engl.* 32 (1993) 882.
- [14] K. Doi, T. Ishida, T. Nogami, *Chem. Lett.* (2003), in press.
- [15] F.M. Romero, R. Ziessel, M. Bonnet, Yl. Pontillon, E. Ressouche, J. Schweizer, B. Delley, A. Grand, C. Paulsen, *J. Am. Chem. Soc.* 122 (2000) 1298.
- [16] O. Kahn, R. Prinz, J. Reedijk, J.S. Thompson, *Inorg. Chem.* 26 (1987) 3561.
- [17] (a) D. Luneau, P. Rey, J. Laugier, P. Fries, A. Caneschi, D. Gatteschi, R. Sessoli, *J. Am. Chem. Soc.* 113 (1991) 1245; (b) D. Luneau, P. Rety, J. Laugier, E. Belorizky, A. Congne, *Inorg. Chem.* 31 (1992) 3578.
- [18] (a) F. Kanno, K. Inoue, N. Koga, H. Iwamura, *J. Am. Chem. Soc.* 115 (1993) 847;

- (b) J. Fujita, M. Tanaka, H. Suemune, N. Koga, K. Matsuda, H. Iwamura, *J. Am. Chem. Soc.* 118 (1996) 9347;
(c) W.T. Borden, H. Iwamura, J.A. Berson, *Acc. Chem. Res.* 27 (1994) 109.
- [19] (a) S. Fang, M.-S. Lee, D.A. Hrovat, W.T. Borden, *J. Am. Chem. Soc.* 117 (1995) 6727;
(b) P. Wautelet, L. Catala, A. Bieber, P. Turek, J.-J. Andre, *Polyhedron* 20 (2001) 1571.
- [20] A. Escuer, S.B. Kumar, M. Font-Bardia, X. Solans, R. Vicente, *Inorg. Chim. Acta* 286 (1999) 62.
- [21] (a) K. Tanaka, M. Kozaki, D. Shiomi, K. Sato, T. Takui, K. Okada, *Abstract Book of the 81st Japan Chemical Society Spring Meeting* (2002) 1249;
(b) H. Kanda, Y. Narumi, Y. Hosokoshi, T. Suzuki, S. Sawata, S. Kawata, K. Kindo, K. Inoue, S. Kaizaki, *Abstract Book of the 81st Japan Chemical Society Spring Meeting* (2002) 487.